Environ Earth Sci (2016)75:1127
DOI 10.1007/s12665-016-5903-z

ORIGINAL ARTICLE

Quantifying the hazardous impacts of human-induced land degradation on terrestrial ecosystems: a case study of karst areas of south China

Degen Lin[1,2] · Han Yu[1,2] · Fang Lian[1,2] · Jing-ai Wang[1,2,3] · A-xing Zhu[4,5] · Yaojie Yue[1,2,3]

Received: 15 April 2015 / Accepted: 18 July 2016

Abstract This paper assesses the harm that human-induced land degradation poses on terrestrial ecosystems. We propose and define a hazardous impact (HI) indicator and a method to quantify this degradation and promote sustainable land use under the pressure resulting from population growth. Taking human appropriation of the net primary productivity owing to land-use conversion ($HANPP_{luc}$) as a proxy, the quantification of HI was developed with support from remotely sensed net primary productivity (NPP) data and using the co-kriging method. A case study in the karst area of south China showed that HI in the study area decreased from southwest to northeast. Areas with the highest level of HI occupied 4.77 % of the total area and were distributed in northwest Sichuan Province, southwest Yunnan Province, and southern Guangxi Autonomous Region. Lower HI areas were mainly located in Hunan Province and Hubei Province. This indicates that land use has a strong impact on karst rocky desertification. To maintain a decreasing trend in HI, a land-use policy must guide human activity. In the karst areas of south China, HI and rocky desertification have similar spatial distribution and intensity. This suggests that HI can effectively reveal adverse effects on the ecosystem due to human-induced land degradation, and that it can potentially be applied to other related issues. We also argue that NPP reduction and HI level do not follow a simple 1:1 relationship, so revisions may be needed when applying the proposed indicator and approach to other regions. This approach also needs to be improved in its accuracy in terms of natural vegetation extraction.

Keywords Hazardous impact indicator · Human-induced land degradation · Terrestrial ecosystem · $HANPP_{luc}$ · Co-kriging · Karst areas in south China

Introduction

Land use alters the structure and functioning of terrestrial ecosystems (Vitousek et al. 1997). Also regarded as the "colonization of terrestrial ecosystems" (Fischer-Kowalski and Haberl 1998; Haberl et al. 2001, 2004a, b; Krausmann et al. 2003), land use is an undeniable leading cause of land degradation (Wessels et al. 2004, 2007). It is estimated that 39–50 % of all land has been transformed or degraded by humanity (Reynolds et al. 2007). Human-induced land degradation has led to hazardous impacts on the service and function of terrestrial ecosystems (Bai et al. 2012; Bridges and Oldeman 1999; Fasona and Omojola 2009; Millennium Ecosystem Assessment 2005; Roberts et al. 1999; UNCCD 1993). The momentum of human population growth has created an urgent need to quantify the hazardous impact of human-induced land degradation on terrestrial ecosystems.

✉ Yaojie Yue
yjyue@bnu.edu.cn

1 School of Geography, Beijing Normal University, Beijing 100875, China

2 Key Laboratory of Regional Geography, Beijing Normal University, Beijing 100875, China

3 State Key Laboratory of Earth Surface Processes and Resource Ecology, Beijing Normal University, Beijing 100875, China

4 Jiangsu Center for Collaborative Innovation in Geographical Information Resource Development and Application and School of Geography, Nanjing Normal University, Nanjing, China

5 Department of Geography, University of Wisconsin-Madison, Madison, WI 53706, USA

Published online: 01 August 2016

To quantify this, we must first distinguish between land degradation caused by human land exploitation and that caused by climatic change on broad spatial scales; yet, there are still few well-established procedures for such an analysis. Recently, residual trend (RESTREND), a relatively new method, has been proposed in several studies for this purpose (Evans and Geerken 2004; Wessels et al. 2007). This method identifies the rainfall period that is most related to the annual maximum NDVI ($NDVI_{max}$) and therefore the proportion of biomass triggered by rainfall, by performing regression calculations between different periods of accumulated precipitation and $NDVI_{max}$; positive or negative deviations in biomass from this relationship, expressed in the residuals, are considered to be human-induced. After arranging the residuals in their temporal order, there is a clear negative trend, indicating an increasingly worse response of the $NDVI_{max}$ to rainfall. This negative trend, if it proves to be statistically significant, indicates an area experiencing human-induced degradation (Evans and Geerken 2004). The RESTREND method is useful for controlling the effects of precipitation in order to detect human-induced land degradation (Wessels et al. 2007) and has been successfully applied in arid or semiarid areas where vegetation production is highly coupled with precipitation (Bai et al. 2008; Li et al. 2012; Wessels et al. 2007). However, it suggests that this NDVI-based method could only be used in arid or semiarid areas, since the NDVI variation is shown to have low relevance to precipitation in rainy areas (Wessels et al. 2007), even though its applicability and effectiveness have not been evaluated beyond arid and semiarid areas. These studies have established the idea that human-induced degradation can be detected by comparing actual vegetation levels with potential levels (Evans and Geerken 2004; Wessels et al. 2007; Zhou et al. 2015).

More recently, human appropriation of net primary productivity (HANPP), an integrated socio-ecological indicator that can be used to quantify human domination of ecosystems (Vitousek et al. 1997) and to understand and map important aspects of land-use intensity, has been developed (Erb et al. 2013; Haberl et al. 2007, 2014; Kuemmerle et al. 2013) and successfully used to detect human-induced land degradation (Haberl et al. 2014; Zhou et al. 2015; Zika and Erb 2009). Changes in NPP resulting from land conversion and land use [i.e., the difference between productivity of potential vegetation (NPP_{pot}) and productivity of actual vegetation (NPP_{act})] are also denoted as $HANPP_{luc}$ (Haberl et al. 2007, 2014; Krausmann et al. 2013). Among the processes that contribute to $HANPP_{luc}$, land degradation is an environmental and developmental issue of global importance (Zika and Erb 2009). Human-induced soil/land degradation leads to substantial levels of $HANPP_{luc}$ (Haberl et al. 2014), commonly resulting in the temporary or permanent reduction in the productive capacity of land (Zika and Erb 2009). Therefore, $HANPP_{luc}$ appears to be more suitable to express the hazardous impacts of human-induced land degradation on terrestrial ecosystems. There is thus a need to quantify its hazardous impact on terrestrial ecosystems (Nel et al. 2014; Nicholson et al. 1998; Wessels et al. 2004), but $HANPP_{luc}$ includes both positive and hazardous aspects (Cao et al. 2014; Plutzar et al. 2016).

Karst terrain accounts for about 15 % of the world's land area, or about 2.2 million km^2, and is where around 17 % of the world's population, or about 1 billion people, live (Xiao and Weng 2007). Ford and Williams (1989) suggested that 25 % of the world's population rely largely or entirely on karst waters, including deep carbonate aquifers. The south China karst area, the Earth's largest, merits the highest international level of protection (Williams 2008), as it is home to about 100 million people (Cai 1996). Rocky desertification, which is caused by complex human land-use activities on the fragile karst ecosystems, induces the most serious land degradation in this area (Xiao and Weng 2007; Xiong et al. 2009). In most cases, human land-use activities, including cultivation, deforestation, grazing, and burning (Tian et al. 2008), play a critical role in rocky desertification (Jiang et al. 2014). Due to the close connection between irresponsible land-use and karst environmental problems, studies of human-induced land degradation in karst areas have received increased attention (Grau et al. 2003; Gutiérrez et al. 2014; Williams 1993; Xiong et al. 2009). Its hazardous impact in this area must be studied if the damaged environment is to be rebuilt and a sustainable ecosystem achieved.

The main goal of this study is to propose an analytic method for quantifying the hazardous impact of human-induced land degradation on terrestrial ecosystems. In the following sections, we will first describe the methodological framework, taking $HANPP_{luc}$ as a proxy. Then, in a case study, the proposed method will be applied to the south China karst region. Last, we will discuss the research findings and shortcomings in detail.

Methodology

Basic idea and research framework

Land degradation has a broad range of definitions, which essentially describe the circumstances of reduced biological productivity (Reynolds and Stafford Smith 2002; UNCCD 1994; Wessels et al. 2004, 2007). Serious land degradation ultimately results in long-lasting and observable loss of vegetation cover and biomass productivity over time and

space (Haboudane et al. 2002; Wessels et al. 2012). Productivity shows significant negative trends when human-induced land degradation is introduced (Wessels et al. 2004, 2007; Xu et al. 2010), so loss of productivity has been widely used to detect and monitor it (de Jong et al. 2011; Prince et al. 2009). We therefore define the *hazardous impact of human-induced land degradation* (denoted as HI), specifically restricted to karst areas, as destruction of terrestrial ecosystem services and functions caused by degradation-induced human land-use activities. More specifically, the destruction of services and functions leads to potential productivity loss. From the perspective of disaster risk science (Blaikie et al. 2014; Burton 1993; Shi 2002), a karst terrestrial ecosystem is a receptor of hazard, while human-induced land degradation is the hazard source. For quantifying HI, three basic hypotheses are put forward:

Hypothesis 1 Because human-induced land degradation (unsustainable land use) ultimately leads to the reduction in potential ecosystem productivity where $HANPP_{luc}$—the difference between NPP_{pot} and NPP_{act} (Haberl et al. 2007, 2014)—is over 0, the ecosystem is affected by human-induced land degradation. Further, where $HANPP_{luc}$ is over 0 and is increasing, the terrestrial ecosystems are experiencing aggravated hazardous impacts caused by human-induced land degradation. The intensity of HI can be expressed quantitatively by Eq. 1.

$$HI = \frac{HANPP_{luc+}}{NPP_{pot}} \quad (1)$$

where $HANPP_{luc+}$ is $HANPP_{luc}$ over 0, and NPP_{pot} is the potential NPP. HI ranges from 0 to 1; a bigger HI means human-induced land degradation has a more hazardous impact on the terrestrial ecosystem.

$HANPP_{luc+}$ is worked out by Eq. 2.

$$HANPP_{luc+} = NPP_{pot} - NPP_{act} \quad (\text{If } NPP_{pot} > NPP_{act}) \quad (2)$$

where NPP_{pot} is the potential NPP, and NPP_{act} is actual NPP.

This hypothesis does not deny that changes in land use, such as from farmland to urban, affect $HANPP_{luc}$. However, the hypothesis fits well with the conditions in the karst area of south China, where human land use dominates the process of land degradation and human-induced land degradation is the main cause of destruction of terrestrial ecosystems (Kiernan 2010; Wang et al. 2004; Williams 1993; Xiong et al. 2009). We also emphasize that this hypothesis should be carefully checked and may need to be revised to adapt to other regions (see "HI, human-induced land degradation and reduction of ecosystem productivity" section).

Hypothesis 2 It is believed that natural vegetation still exists in protected areas, according to the research by Hobbs and Harris (2001). Natural vegetation is vegetation that exists under current environmental conditions and without disturbance from human activities, according to Niche (Hutchinson 1965) and restoration ecology (Hobbs and Harris 2001).

In this case, natural vegetation is defined as vegetation that is distributed in world and national protected zones. The methods for obtaining natural vegetation are described in "Natural vegetation extraction" section.

Hypothesis 3 The potential productivity is equal to current actual productivity if the vegetation remains undisturbed by human land use, that is, NPP_{pot} equals NPP_{act} in non-degraded areas.

Further, according to Tobler's first law of geography (Tobler 1970), the potential productivity of degraded areas should be equal or similar to that of natural vegetation regions when the degraded and non-degraded areas have identical or similar natural conditions. If the non-degraded, potential production of the land can be inferred, the condition of the rest of the land can be mapped relative to this NPP (Boer and Puigdefabregas 2003; Wessels et al. 2008). Therefore, if NPP_{act} of natural vegetation is known, then regional NPP_{pot} can also be predicted in degraded areas, taking most correlative natural factors as co-variables.

In this case, MODIS MOD17A3 NPP in a natural vegetation area was taken as reference data, and the co-kriging method (Couckuyt et al. 2013; Kennedy and O'Hagan 2000) was adopted to predict NPP_{pot} in other areas. The methodologies for predicting NPP_{pot} are described in "Potential productivity prediction using the co-kriging method" section.

In summary, quantifying the hazardous impact of human-induced land degradation on a terrestrial ecosystem is done in three general steps (Fig. 1): (1) extraction of natural vegetation data based on local land-use data, (2) prediction of potential productivity using the co-kriging method, and (3) calculation of HI.

Procedures for calculating HI are shown in Eqs. 1 and 2. The methodology for obtaining natural vegetation and predicting NPP_{pot} is described in the following sections.

Natural vegetation extraction

The types and characteristics of natural vegetation show a regional difference because of different natural circumstances. Therefore, natural vegetation data should be extracted for each site.

In order to ensure the representativeness of natural vegetation in our study areas, where the primitive vegetation is forest (Ramankutty and Foley 1999; Ray and Adams 2001), a metric of tree height was introduced. Zeng et al.

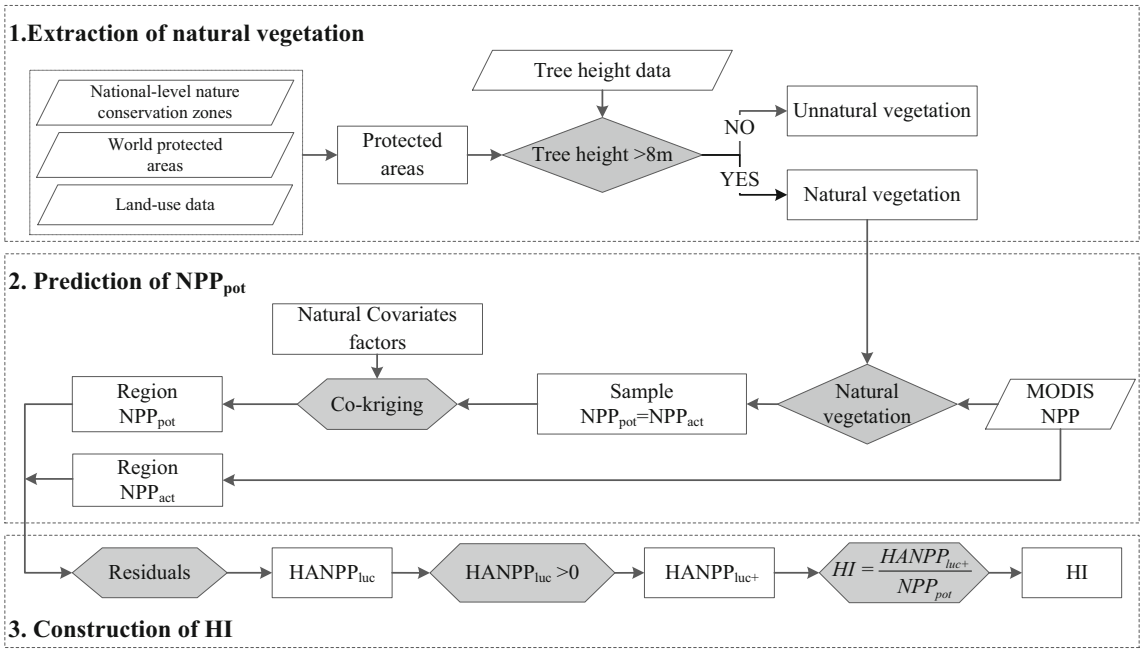

Fig. 1 Basic concept for quantifying $HANPP_{luc}$-based hazardous impacts caused by human-induced land degradation

(2007) pointed out that secondary forest in degraded areas has lower tree heights than primitive forest because of thin and infertile soil caused by human-induced land degradation. Liu et al. (2009) and Du et al. (2013) observed that vegetation was significantly degraded in unprotected areas and that tree height was far lower than in protected areas. According to Zeng et al. (2007) and Du et al. (2013), the height of trees in primitive forests was over 8 meters in protected areas but generally < 5 m in degraded areas. Therefore, 8 meters of tree height was introduced as a threshold to extract natural vegetation.

With the support of databases of world protected areas (IUCN and UNEP-WCMC 2015), national-level nature conservation zones (State Forestry Administration of China 2013), a land-use map of the study area (Friedl et al. 2010), and tree height data distributed by NOAA (Simard et al. 2011), natural vegetation can be extracted by applying a threshold of 8 meters.

Potential productivity prediction using the co-kriging method

Co-kriging (Kennedy and O'Hagan 2000) is a type of kriging in which the correlation between the high-fidelity model and the low-fidelity model is exploited to enhance prediction accuracy (Couckuyt et al. 2013). It is appealing because it takes important natural factors into consideration as covariates (Gong et al. 2014). Two steps are needed when using the co-kriging method.

Correlative analysis between NPP_{pot} and natural factors

The relationship between NPP and natural factors was analyzed by Pearson's correlation analysis (Eq. 3):

$$r = \frac{\sum (X - \bar{X})(Y - \bar{Y})}{\sqrt{\sum (X - \bar{X})^2 \sum (Y - \bar{Y})^2}} \quad (3)$$

where r is the correlation coefficient, X is the NPP value, $\bar{X}$ is the mean NPP, Y is some natural factor, and $\bar{Y}$ is the mean value of the natural factor. The correlation coefficient is between -1 and 1. The higher the correlation coefficient value, the greater the impact on NPP.

The total contribution of the temperature, precipitation, and solar radiation to NPP variation is 85 % (Liu et al. 2014), and relative humidity can also significantly alter the magnitude of NPP (Pan et al. 2014). Thus, temperature, precipitation, solar radiation, and relative humidity were selected as natural factors. Sunshine hours were used in this study instead of solar radiation, since solar radiation was not recorded in the study area. The temperature, precipitation, sunshine hour, and relative humidity data from every weather station were transformed into raster data by the kriging interpolation tool in ArcGIS.

Using co-kriging to predict NPP_{pot}

The colocated co-kriging estimator (Wang et al. 2013) is written by Eq. 4:

$$Z_{\mathrm{OCK}}^{(1)^*}(u) = \sum_{a_1=1}^{n_1(u)} \lambda_{a_1}^{\mathrm{OCK}}(u) Z_1(u_{a_1}) + \sum_{i=2}^{N_v} \lambda_i^{\mathrm{OCK}}(u)[Z_i(u) - m_i + m_1] \quad (4)$$

with the single constraint that all weights must sum to one (Eq.5):

$$\sum_{a_1=1}^{n_1(u)} \lambda_{a_1}^{\mathrm{OCK}}(u) + \sum_{i=2}^{N_v} \lambda_i^{\mathrm{OCK}}(u) = 1 \quad (5)$$

where $Z_{\mathrm{OCK}}^{(1)^*}(u)$ is the predicted $\mathrm{NPP_{pot}}$ value primary variable Z_1 at an unknown location u; $Z_1(u_{a_1})$ are the measured $\mathrm{NPP_{pot}}$ values of the primary variable within the neighborhood of location u; $\lambda_{a_1}^{\mathrm{OCK}}(u)$ refers to the weights associated with each of the measured $\mathrm{NPP_{pot}}$ values of the primary variable; N_v is the total number of variables including the primary variable and secondary variables; $Z_i(u)$ is the colocated datum of the ith secondary variable; $\lambda_i^{\mathrm{OCK}}(u)$ is the weight of the colocated datum of the ith variable; m_1 and m_i are the overall means of the primary variable and the ith secondary variable, respectively. Weights were calculated by using the colocated co-kriging equation system, which was omitted here.

Data sets

Data sets used in this study are shown in Table 1.

The MODIS MOD17A3 NPP, a NASA product from 2000 to 2013, is widely used to assess the $\mathrm{NPP_{act}}$ of ecosystems by land use/land cover (Conijn et al. 2013; Indiarto and Sulistyawati 2014) and was adopted to represent the $\mathrm{NPP_{act}}$ of natural vegetation. This improved MODIS primary production data set is now widely used for monitoring ecological conditions, natural resources, and environmental changes (Zhao et al. 2005).

Case study

Description of study area

The study area (Fig. 2) is the 452,000 $\mathrm{km^2}$ karst region (State Forestry Administration of China 2012) located in south China, containing Guizhou Province, Yunnan Province, Sichuan Province, Guangxi Autonomous Region, Guangdong Province, Hunan Province, Hubei Province, and Chongqing City. This area is located in a tropical monsoon climate and subtropical monsoon climate zone with an annual precipitation of 1000–2200 mm and annual temperature of 16–22 °C. The average NPP is 610–680 gC $\mathrm{m^{-2}\ a^{-1}}$. Due to irrational land use, NPP has regional differences that vary from 0 to 1300 gC $\mathrm{m^{-2}\ a^{-1}}$ (Huang et al. 2013). In 2012, the population density was 217 persons per $\mathrm{km^2}$, which was 152 % of the national population density (State Forestry Administration of China 2012). The cultivated land per capita is 0.08 ha for the whole area and 0.033 ha in some counties with intensive desertification. An estimated 40 % of the land is cultivated. The population and land use are increasing, resulting in severe

Table 1 Data sets

Data name	Contents	Data sources (organization and Web site link)
Study area	Karst region Vector file	The carbonate rock outcrops originate from the World Map of Carbonate Rock Outcrops v3.0, University of Auckland, http://web.env.auckland.ac.nz/our_research/karst/
LUCC data	Evergreen forest, deciduous forest, and mixed forest. 1 km × 1 km, 2000	MOD12Q1, https://lpdaac.usgs.gov/products/modis_products_table/mcd12q1
	Forest rehabilitation data, 2002–2012	China Forestry Statistical Yearbook, State Forestry Administration of China
Vegetation	Height of trees, raster, 1 km × 1 km	NOAA. http://www.nasa.gov/topics/earth/features/forest20120217.html
Protected area	National-level nature conservation zones, vector file, 2013	State Forestry Administration of China. http://www.gov.cn/test/2012-04/18/content_2116472.htm; http://www.forestry.gov.cn/portal/slgy/s/2445/content-684347.html
	World protected areas, vector file, 2013	The World Database on Protected Areas, IUCN and UNEP, http://www.protectedplanet.net/search
NPP data	MODIS MOD17A3 NPP, Raster, 1 km × 1 km, 2000–2013	Numerical Terradynamic Simulation Group (NTSG).University of Montana. ftp://ftp.ntsg.umt.edu/pub/MODIS/NTSG_Products/MOD17/GeoTIFF/MOD17A3/GeoTIFF_30arcsec/
Climate	Temperature, precipitation, sunshine hours, relative humidity, monthly data from 752 weather stations, 2000–2013	National Meteorological Information Centre, http://cdc.cma.gov.cn/home.do

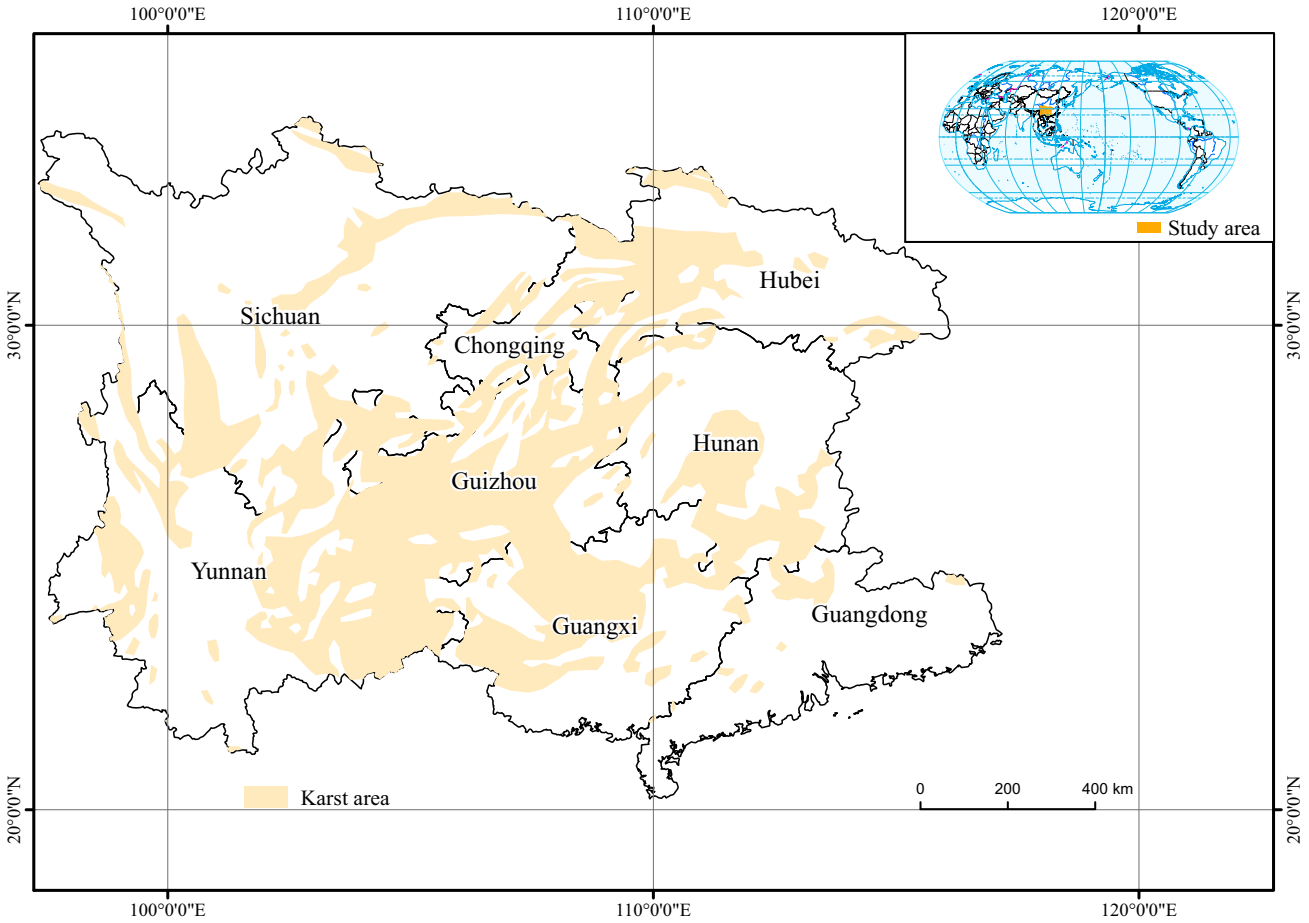

Fig. 2 Study area

rocky desertification. The karst area of Guizhou, Yunnan, and Guangxi Provinces is 8,876,000 km^2 and is 66.2 % of the national karst area (Liu et al. 2009).

NPP_{pot} in karst areas of south China

Distribution of natural vegetation

The distribution of natural vegetation in the karst area of south China is shown in Fig. 3.

There were 8485 natural vegetation samples, and all of them were located in world protected areas and national-level nature conservation zones.

NPP_{pot} in karst areas of south China

The correlation of natural factors with NPP_{pot} Correlation coefficients between NPP_{pot} and annual precipitation, annual relative humidity, annual average temperature, and annual sunshine hours in natural vegetation are shown in Table 2 for 2000–2013.

Table 2 shows that, for 2000–2013, when the average temperature was higher than the annual average temperature, the dominant factors were sunshine hours, annual precipitation, and annual mean temperature, and when the average temperature was lower than the annual average temperature, the dominant factors were sunshine hours, annual precipitation, and annual mean humidity. According to Liu et al. (2014), cold temperatures can cause a sudden decrease in NPP. Therefore, in high-temperature years, we used co-kriging with sunshine hours, annual precipitation, and annual mean temperature as co-variables to construct the model to predict NPP_{pot}. In low-temperature years, we used co-kriging with sunshine hours, annual precipitation, and annual mean humidity as co-variables to construct the model to predict NPP_{pot}.

NPP_{pot} prediction validation Leave-one-out cross validation (Fig. 4) was applied to validate the results of predicted NPP_{pot}.

Figure 4 shows that the adoption of the co-kriging interpolation in high-temperature and low-temperature

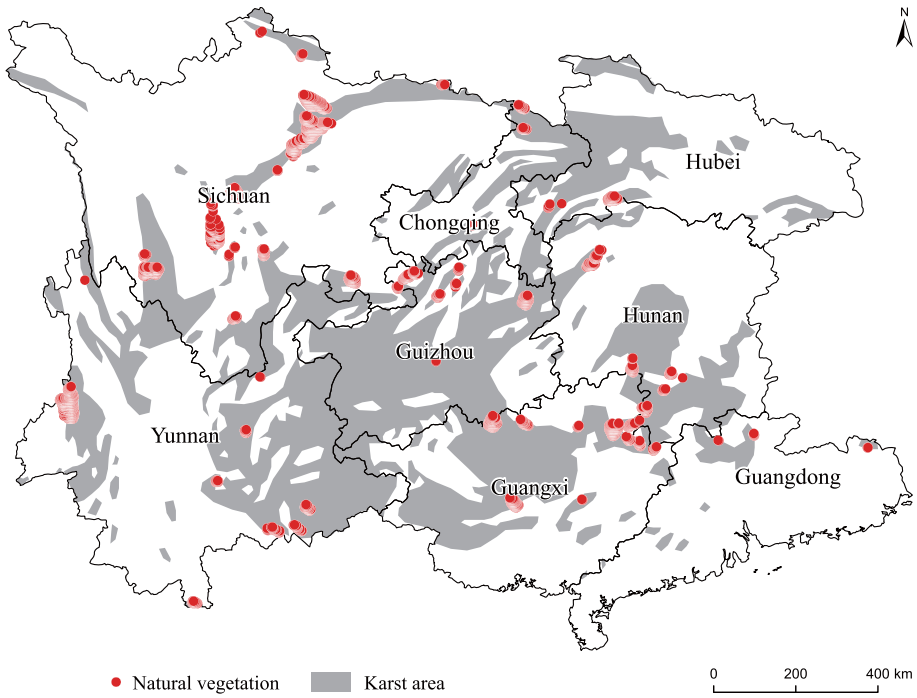

Fig. 3 Distribution of natural vegetation

years satisfied the needed precision. Figure 4a shows that the predicted NPP_{pot} results are on average 0.41 gC m^{-2} a^{-1} lower than the real NPP_{pot}. The points are in a concentrated distribution, and the fit degree is 0.694. Most values of real NPP_{pot} and predicted NPP_{pot} of primary forests are approximately 400 gC m^{-2} a^{-1} and are in line with the productivity of primitive forests in the study area. From Fig. 4b, the predicted NPP_{pot} results are on average 0.3 gC m^{-2} a^{-1} lower than the real NPP_{pot}. The points are in a concentrated distribution, and the fit degree is 0.722. Most values for the real NPP and predicted NPP of primary forests are approximately 400 gC m^{-2} a^{-1} and are in line with the productivity of primitive forests in the study area. Above all, the accuracy of the NPP_{pot} of the study area satisfied the needed precision.

Spatial distribution of NPP_{pot} in karst areas of south China NPP_{pot} in karst areas of south China from 2000 to 2013 was obtained (Fig. 5).

There are few yearly differences in NPP_{pot}; it is higher in the southwest and lower in the northeast. Yunnan, southern Guangxi, and southern Guangdong had the highest potential NPP; Guizhou and southern Sichuan had moderate potential; and Hubei, Hunan, and Chongqing had the lowest. The reason for this pattern is that the southwestern region is nearly covered in virgin forest. Most of the original forest is evergreen broadleaf forest, and the NPP of evergreen broadleaf forest is higher than other vegetation (Huang et al. 2013). The NPP of primary forest has a negative correlation with longitude and latitude and positive correlation with sunshine, so in the southwest area of study, the NPP also had a high value. The value of NPP_{pot} was highly variable in east Yunnan and Guizhou, especially in the eastern region of Yunnan, which had a three-year drought from 2009 to 2011, causing severe damage to vegetation (State Forestry Administration of China 2012). In this area, NPP_{pot} was probably influenced by natural factors.

HI in karst areas of south China

Spatial distribution of HI

HI was classified into nine grades (Jiang 2013): <0.05, 0.05–0.1, 0.1–0.2, 0.2–0.25, 0.25–0.3, 0.3–0.35, 0.35–0.4, 0.4–0.5, and >0.5. The annual average HI from 2000 to 2013 is shown in Fig. 6a. The proportion of HI in different provinces is shown in Fig. 6b.

Figure 6a, b shows that the HI of the study area was unevenly distributed. The study area with HI between 0 and 0.05 was the largest, at 43.47 % of the total area, while the area between 0.1 and 0.2 was 13.98 %. The area between 0.4 and 0.5 was 6.4 %, and the area above 0.5 was 4.77 %. HI in the study area decreased from southwest to northeast. The area with the highest HI was located in northwest Sichuan Province, southwest Yunnan Province, and southern Guangxi Autonomous Region. Moderate HI was located in southwest Guizhou Province. Lower HI areas were in Hunan Province and Hubei Province.

The pattern of HI in south China is consistent with karst rocky desertification (KRD) in south China. Some studies

Table 2 Pearson's correlation coefficients between NPP_{pot} and natural factors in natural vegetation area

Element	Year												
	2000	2001	2002	2003	2004	2005	2006	2007	2008	2009	2010	2011	2012	2013
Precipitation	0.09**	0.30**	−0.13**	−0.13**	0.14**	−0.14**	−0.23**	0.00	−0.20**	−0.25**	0.09**	−0.19**	−0.05**	−0.24**
Relative humidity	0.06**	0.02	−0.12**	0.00	−0.22**	−0.32**	−0.11**	0.02	−0.01	−0.23**	−0.21**	−0.04**	−0.14**	−0.12**
Sunshine hours	0.35**	0.41**	0.44**	0.41**	0.38**	0.58**	0.54**	0.40**	0.50**	0.50**	0.62**	0.69**	0.60**	0.55**
Temperature	0.04**	0.00	0.00	−0.02*	−0.17**	−0.09**	−0.24**	−0.20**	−0.18**	−0.18**	−0.11**	−0.18**	0.03**	−0.11**

* Significance level of 0.05

** Significance level of 0.01

(Jiang et al. 2014; Sweeting 2012) have found that in south China, Yunnan had severe KRD and Guizhou had moderate rocky desertification. The distribution of HI followed the same pattern. Specifically, the pattern of HI in Guizhou was similar to the degree of KRD. Using the KRD land data from Bai et al. (2013), we found a relationship KRD land with HI in Guizhou (Table 3).

As shown in Table 3, the percentage of KRD land, which was found by Bai et al. (2013) in 2000, was similar to the percentage of HI in Guizhou. The root mean square error (RMSE) for the percentage of KRD and the percentage of HI is 4.25. In lower KRD areas, where there is little KRD or potential KRD land, the percentage of KRD was smaller than the percentage of HI, and the RMSE was 5.88. The error was larger than average because area with the lower KRD was affected by both natural and human activities. However, in areas with moderate, severe, and extreme KRD, the percentage of KRD was quite close to the percentage of HI, and the RMSE was 1.23. Human activity was the dominant factor in higher KRD areas, so HI was a good estimator and could be used to explain KRD areas highly affected by human activities.

HI may change due to rapid economic development and intensive land-use/land-cover change (Sorrensen 2009). In China, the Grain-for-Green Project was in effect from 2000 to 2010 (Lei et al. 2012; Uchida et al. 2005) as a policy to alleviate severe land degradation problems (Lei et al. 2012; Wang et al. 2007; Li 2004), and it reestablished the terrestrial ecosystem through human activity. As its completion in 2010, the projects had converted 14.67 million ha of farmland into forestland and grassland, and participants had planted trees on 17.3 million ha of barren mountains and lands suitable for afforestation. It thus greatly improved natural environments across China and made significant progress in afforestation. In order to find the relationship between HI and afforestation, we calculated annual HI per province from 2000 to 2013 (Fig. 7a) and compared annual HI with the annual afforestation ratio (total afforestation area/total counties area) (Fig. 7b).

In Fig. 7a, the linear trend shows that HI decreased, but that the reduction was not severe. The decreasing coefficient is −0.002, and the fit degree is 0.28. The annual mean HI of the study area fluctuated from 0.13 to 0.22, and each province fluctuated between 0.03 and 0.27. The annual mean HI of Yunnan was the highest, and Chongqing was the lowest. Figure 7b shows that HI had a wavelike reduction, and the afforestation ratio rose from 2000 to 2013. This suggests that the negative effects of human activities on ecosystems weakened, and the positive effects were enhanced. HI decreased in most provinces from 2000 to 2008, which means ecosystems improved. These increases were due to the forest rehabilitation policy and indicated that afforestation on a large scale will reduce the

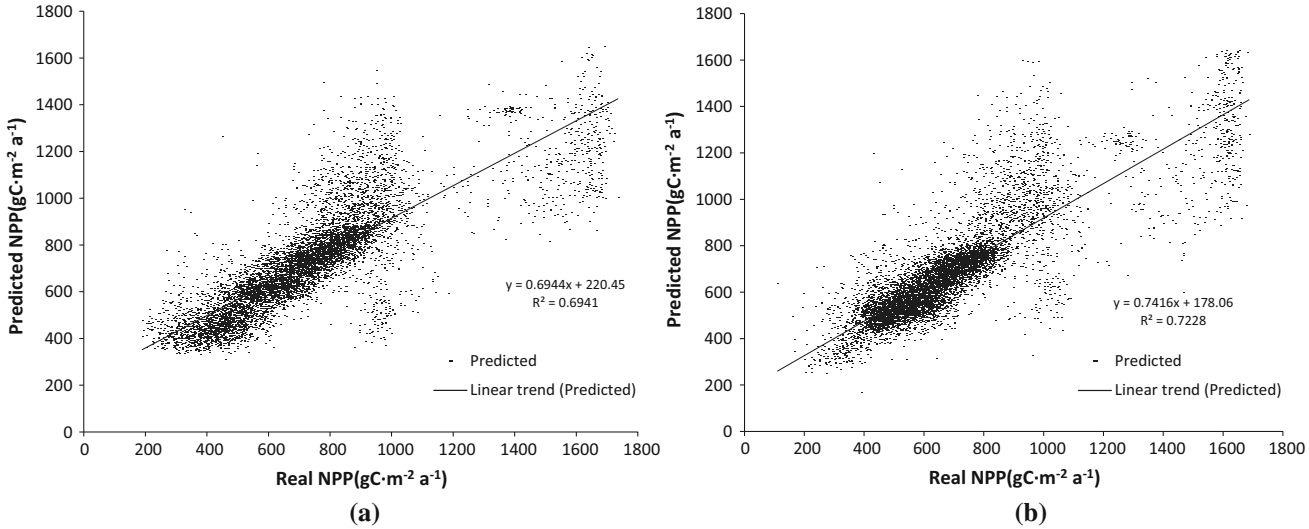

Fig. 4 Leave-one-out cross-validation results. **a** High-temperature year (2009), **b** low-temperature year (2012)

negative effect of human activities on ecosystems. However, from 2008 to 2010, the afforestation ratio increased despite an increase in HI. Investment in the Grain-to-Green Project was the least in 2008, delaying the improvement of the ecosystem, so HI increased after 2008. When the afforestation ratio continued increasing in 2011 and reached its climax, HI dropped significantly. Above all, the change in HI is related to afforestation.

Spatial variation in HI with human-induced land degradation

In order to study the spatial variation in HI, we compared HI in the year when the Grain-to-Green Project reached its climax and HI dropped significantly (2011), when the Grain-to-Green Project started (2000), and the most recent year (2013). The result is shown in Fig. 8.

Figure 8 shows that low-HI areas expanded and high-HI areas shrank from 2000 to 2011 and that low-HI areas shrank and high-HI areas expanded from 2011 to 2013. The proportion of areas with HI <0.05 was 41.65 % in 2000, 53.87 % in 2011, and 47.23 % in 2013. The proportion of areas with HI >0.4 was 16.59 % in 2000, 11.81 % in 2011, and 12.23 % in 2013.

From 2000 to 2011, high-HI area decreased yearly and low-HI area expanded. The HI increased in Yunnan from 2000 to 2011 in high-HI areas. The growth of HI area between 0.4 and 0.5 was 17.17 %, and the growth of HI area >0.5 was 14.54 %. HI decreased in Guizhou from 2000 to 2011 in low-HI areas; it reduced 9.07 % in areas with HI between 0.25 and 0.3, 24.08 % in areas with HI between 0.3 and 0.35 and 29.14 % in areas with HI between 0.35 and 0.4 compared with 2000. This means that the ecological environment improved. This may be the result of the Grain-to-Green Project, which led to a large amount of reforestation (Qi et al. 2013). However, in 2011-2013, the high-HI area increased. HI decreased in Yunnan from 2011 to 2013: 8.82 % in areas with HI between 0.4 and 0.5 and 8.18 % in areas with HI >0.5. HI increased in Guizhou from 2011 to 2013: 14.84 % in areas with HI between 0.25 and 0.3, 12.3 % in areas with HI between 0.3 and 0.35, and 8.01 % in areas with HI between 0.35 and 0.4 compared with 2011. This is consistent with year in which the Grain-for-Green Project ended in 2010, implying that the Grain-for-Green Project had a strong impact on HI.

Factors driving the HI of human-induced land degradation

HI appears to have been highly influenced by the Grain-for-Green Project. The change slope from 2000 to 2013 for HI is shown in Fig. 9a. The total afforestation area per county from 2002 to 2012 was calculated from the data in Table 1 (Fig. 9b). A Pearson's correlation analysis was used to study the relationship between the afforestation ratio and total afforestation area and between the average and total HI (Table 4).

The Grain-for-Green Project had a strong impact on HI spatially. Figure 9a shows that the spatial variation trend of HI was lower in the middle of the study area (mostly west Guizhou). In the same location, Fig. 9b shows that the total afforestation area was correspondingly higher. The spatial variation trend of HI was higher in the northwestern and southern regions of the study area, as shown in Fig. 9a. In summary, the size of the forest area correlates in space with the variation trends of HI. This is consistent with the conclusions of the China Rocky Desertification Communique (State Forestry Administration of China 2012). The

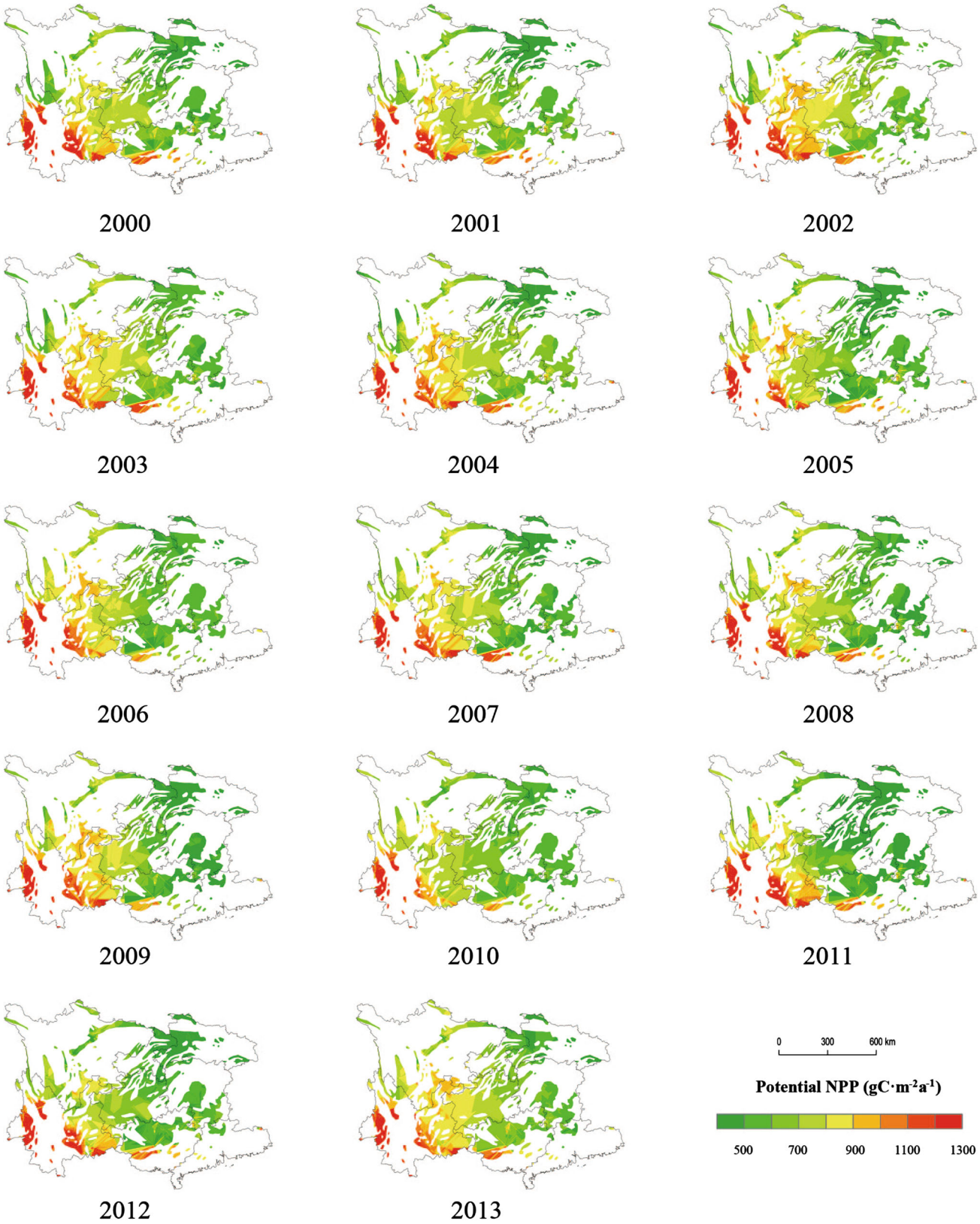

Fig. 5 NPP_{pot} of study area in 2000–2013

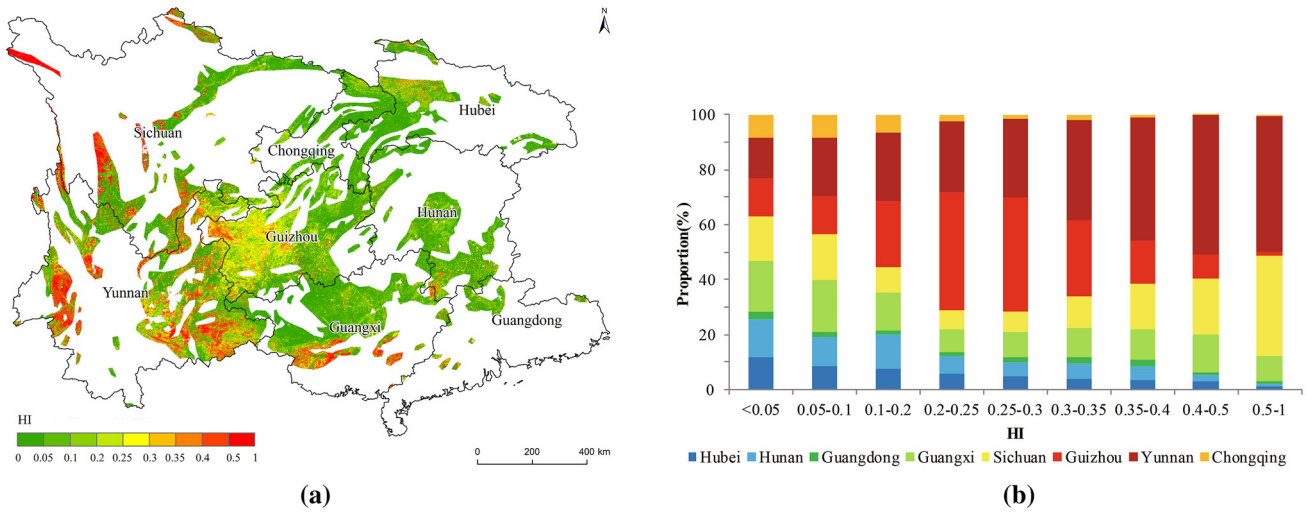

Fig. 6 **a** Annual mean HI from 2000 to 2013. **b** Proportion of HI in different provinces

Table 3 Percentage of KRD land and corresponding HI in Guizhou Province

Type of karst rocky desertification (KRD) land	Percentage of KRD (%)	Grade of HI	Percentage of HI (%)
No KRD	35.38	<0.05, 0.05–0.1	39.18
Potential KRD	29.07	0.1–0.2, 0.2–0.25	33.97
Light KRD	21.65	0.25–0.3	13.57
Moderate KRD	11.86	0.3–0.35, 0.35–0.4	9.98
Severe KRD	2.01	0.4–0.5	2.95
Extremely KRD	0.02	0.5–1	0.35

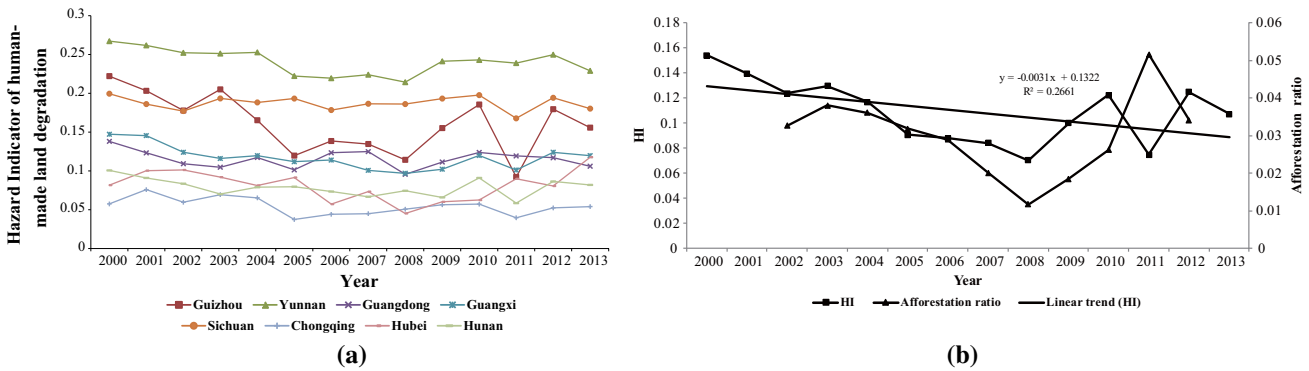

Fig. 7 **a** HI variation per province from 2000 to 2013. **b** Relationship between HI and afforestation

Grain-to-Green Project mitigated the intensity of rocky desertification to some extent.

The results show that the afforestation ratio is significantly and negatively correlated with HI at the 0.01 level and that the correlation coefficient is −0.209. The total afforestation area is negatively correlated with total HI at the 0.01 level, and the correlation coefficient is −0.29, showing that the Grain-to-Green Project had a negative correlation with HI. Zhang et al. (2014) suggested that the Grain-to-Green Project accelerated land-cover transition in Yunnan and reduced HI in the ecosystem. This matches findings from other regions of southwest China (Brandt et al. 2012). In addition, karst landscapes were in a fluctuating state of restoration because of the implementation of ecological construction projects (Yue et al. 2013). Therefore, both previous studies and our results illustrate that by human land-use activities have a strong impact on HI. To continue this decreasing HI trend, land-use policies are strongly recommended.

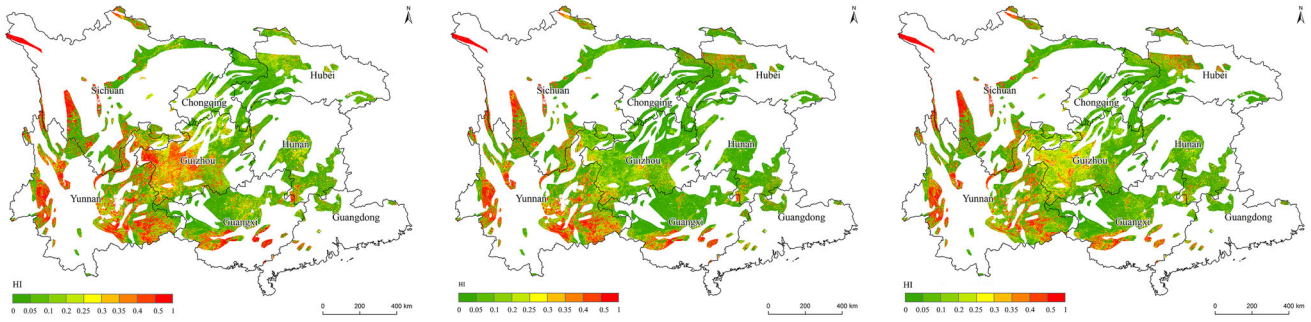

Fig. 8 Annual HI in study area. **a** 2000, **b** 2011, **c** 2013

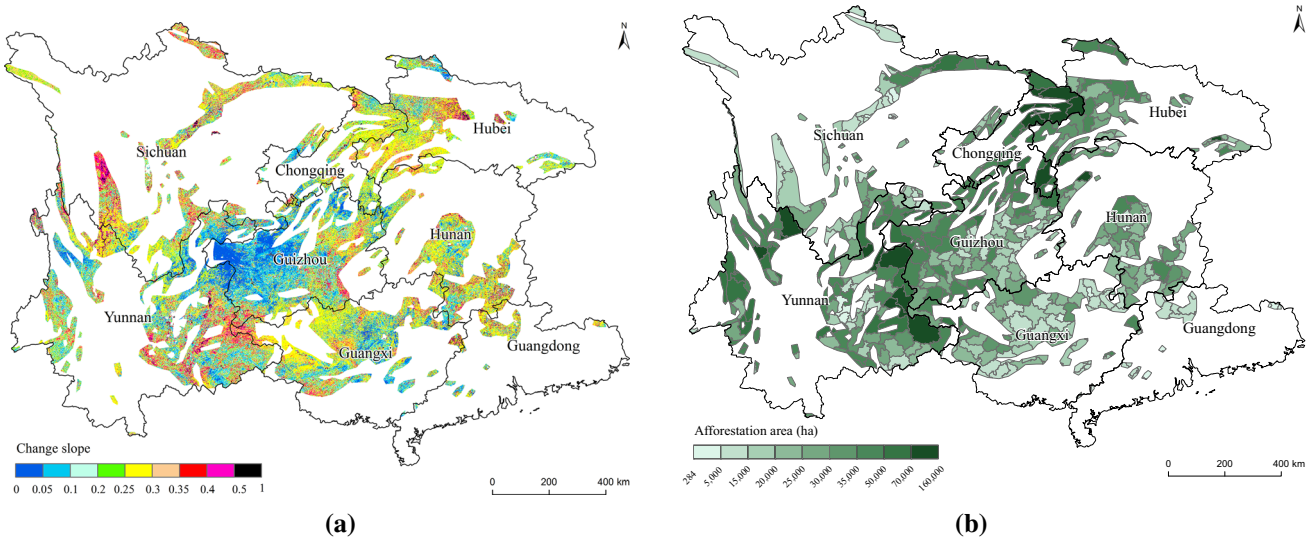

Fig. 9 **a** Change slope of HI from 2000 to 2013 and **b** total afforestation area per county from 2002 to 2012

Table 4 Pearson's correlation coefficient of HI and afforestation ratio

	Total afforestation area	Afforestation ratio
Average HI	−0.114**	−0.209**
	0.008	0.000
	530	530
Total HI	−0.290**	−0.035
	0.000	0.418
	530	530

** Significant at $p < 0.01$ level (two-tailed)

Discussion

HI, human-induced land degradation, and reduction in ecosystem productivity

This paper proposed a new indicator, HI, to quantify the hazardous impacts of human-induced land degradation on terrestrial ecosystems. The core meaning of this indicator is based on the fact (Reynolds and Stafford Smith 2002; UNCCD 1994; Wessels et al. 2004, 2007) that human-induced land degradation ultimately leads to a reduction in terrestrial ecosystem productivity. Thus, the damaging impact of human-induced land degradation can be measured by comparing NPP before and after degradation, that is, $NPP_{act} - NPP_{pot}$ (Haberl et al. 2007, 2014; Krausmann et al. 2013). This hypothesis fits with the process and consequences of human-induced degradation that occurred in the past and also coincides with currently occurring

degradation in karst areas in south China (Kiernan 2010; Wang et al. 2004; Williams 1993; Xiong et al. 2009). While the definition does not explicitly claim that a reduction in NPP results from human-induced land degradation, it does not deny that an increase in NPP has no hazardous impact. That is, NPP reduction and HI level do not have a 1:1 relationship.

In addition to land degradation, there are other human activities that can lead to a reduction in NPP, which in turn results in a higher $HANPP_{luc}$. Several processes contribute to $HANPP_{luc}$: changes in NPP due to (1) changes in land cover, such as clearing pristine ecosystems for agricultural purposes (Haberl et al. 2014; Monfreda et al. 2008) or soil sealing by construction of infrastructure and settlement areas and (2) modifications of ecosystem patterns and processes without changing land cover (i.e., within-land-cover changes), such as changes in NPP caused by modification of vegetation structure, species composition, or soil fertility (Zika and Erb 2009). Moreover, the NPP of agro-ecosystems may be lower than the NPP of potential natural vegetation without implying an unsustainable condition (Haberl et al. 2014; Monfreda et al. 2008), though up to 40 % of global croplands may also be experiencing some degree of degradation (Foley et al. 2005). Consequently, although a reduction in NPP is used to detect and quantify the extent and rate of degradation (Diouf and Lambin 2001; Prince et al. 1998; Prince 2002; Wessels et al. 2004, 2008), not all reductions in NPP are an indication of degradation (Zika and Erb 2009).

On the other hand, an increase in NPP does not mean that there are no hazardous impacts. The application of new technologies has become one of the most important direct drivers of changes in ecosystem productivity (Millennium Ecosystem Assessment 2005). NPP can be raised over NPP_{pot} with the use of technologies that may jeopardize future soil or ecosystem quality, e.g., through high input of mineral fertilizers (Haberl et al. 2014). However, a large portion of croplands, up to 40 % globally, according to Foley et al. (2005), is not sustainable. Although the effects of land degradation on productivity can sometimes be compensated for with increased fertilization or irrigation (Tilman et al. 2002), this may have high costs in terms of energy input and ecological pressure, such as nutrient leaching or soil degradation (Haberl et al. 2014). That is, the onset of degradation is often masked by intensification of land use; intensification usually exacerbates degradation to maintain productivity on degraded soils (Daily 1995; Tilman et al. 2002), which may eventually result in a reduction in NPP later on. Therefore, modern land-use practices, while increasing short-term supplies of material goods, may undermine many ecosystem services in the long run, even on regional and global scales (Foley et al. 2005), which reinforces the need for more sustainable agricultural methods (Tilman et al. 2002).

Nevertheless, NPP reduction and HI do not have a simple 1:1 relationship. Many factors and human activities may cause NPP change, and the relationship between NPP reduction and human-induced land degradation is complex. Therefore, some studies have emphasized that although NPP reduction can be used to detect land degradation, more fieldwork is needed to determine the specific causes of NPP reduction (Prince et al. 1998; Prince 2002; Wessels et al. 2004, 2008; Haberl et al. 2014). In some areas, human activities contribute only a small portion of NPP reduction, e.g., 24 % of yearly potential NPP (based on the year 2000) (Haberl et al. 2007). We also argue that, in some fragile ecological environment areas, unsustainable human land use, which ultimately leads to land degradation, may play a key role in terrestrial ecosystem degradation and eventually lead to significant NPP reductions. For example, under karst conditions, strong reductions of NPP in many cases are indicative of degradation effects (Kiernan 2010; Wang et al. 2004; Williams 1993; Xiong et al. 2009). Human land use plays an especially critical role in the rocky desertified area (Jiang et al. 2014; Tian et al. 2008; Xiao and Weng 2007; Xiong et al. 2009) in the south China karst region, the world's largest karst area, which has a dense population (Cai 1996). In this region, due to the characteristics of mountainous topography, sloping cultivation is widely applied. Sloping cultivated land accounts for 70 % of the total cultivation area, and 20 % of land has a slope larger than 25° (Huang et al. 2008). Such high intensity of sloping farming has destroyed the original vegetation, resulting in serious soil erosion, forming a large area of rocky desertification and ultimately reducing the NPP significantly (Bai et al. 2013; Huang et al. 2013). In this area, the significant reduction in NPP is as an irrefutable indicator of degradation effects. We therefore hypothesize that $HANPP_{luc+}$ could be an indicator to reveal the hazardous impacts of human-induced land degradation posed on terrestrial ecosystems. The results also show that HI can indicate the distribution and intensity of land degradation caused by human land use in the south China karst area. We also emphasize that this hypothesis should be carefully checked and may need to be revised to adapt to other regions.

It is important that we meet the challenge of developing strategies that reduce the negative environmental impacts of land use across multiple services and scales while maintaining social and economic benefits (Foley et al. 2005). HANPP, an area-specific approach, can serve as an indicator of land-use intensity, gauging impacts on terrestrial ecosystems in a defined area (Haberl et al. 2014). This concept can also be extended to other aspects of ecosystems (Haberl et al. 2004b). This paper attempts to construct a HANPP-based hazardous impact indicator to characterize negative aspects of human activities posed on terrestrial ecosystems. This is only a small step, but we hope to conduct deeper related research in the future.

Uncertainty in predicting NPP_{pot}

Natural vegetation extraction

There is a large body of research that has examined vegetation types prior to human impact in the study area. Nicolas Ray and Adams (2001) found that most vegetation in the area was forest and the rest was shrub (25,000–15,000 B.P.). Ramankutty and Foley (1999) pointed out that the natural vegetation of the study area in the 1700s was forest. This paper assumes that the natural vegetation of the study area was forest.

Most, but not all, of the study area where there is no human interference is covered with forest. Thus, the primitive forest that was used to estimate potential NPP may be too large. Primary forest sample points showed an uneven distribution; there are fewer sample points in the northeastern and southwestern regions. Consequently, the NPP_{pot} spatial interpolation results in the northeast and southwest may have errors.

Comparing the method to predict NPP_{pot}

Some potential NPP models, such as the Miami, Thornthwaitc, and Chikugo models (Lieth 1975), are based on climate factors such as annual average temperature and precipitation (Peng et al. 2007). However, it is difficult to obtain actual NPP data to verify the accuracy of NPP_{pot} when using these models for the calculation. The potential productivity of natural vegetation should equal its current actual productivity, so we used spatial interpolation methods based on the NPP of natural vegetation to predict NPP_{pot}. This study used three spatial interpolation methods: IDW, ordinary kriging, and co-kriging (Alves et al. 2013). The power of IDW is set from 1 to 4 and ordinary kriging and co-kriging choose a stable optimization model, spherical optimization model, exponential optimization model, and Gaussian optimization model.

The fit of each prediction was assessed using five cross-validation parameters (Johnston et al. 2001; Scattolin et al. 2008): the mean prediction error (ME), the root mean square prediction error (RMS), the average standardized prediction error (ASE), the mean standardized prediction error (MS), and the root mean square standardized prediction error (RMSS). The expectations for a spatial interpolation model with a good fit are average ME and MS prediction error close to 0, RMSS prediction error close to 1, a small RMS error and an ASE close to RMSS prediction error (Scattolin et al. 2008). The results are shown in Table 5.

As shown in Table 5, compared with IDW and ordinary kriging, co-kriging with the spherical optimization model has the best fit in the spatial interpolation and has the best ability to predict the NPP_{pot} both in high-temperature (H) and low-temperature (L) years. The RMS and ASE values were similar when using co-kriging to interpolate. This demonstrates that the model accurately represents the variability of the data; the MS value showed a good fit and was close to zero, indicating a rather small error in the estimation of NPP_{pot} predicted values. The RMSS value, close to the optimum value of 1, showed a good fit of the model's predicted values with the data that were collected (Scattolin et al. 2013). According to Johnston et al. (2001), if RMSS <1 or ASE $>$ RMS, there is a tendency toward

Table 5 Validation of different methods to predict NPP_{pot}

Model	ME		RMS		ASE		MS		RMSS	
	H	L	H	L	H	L	H	L	H	L
IDW										
Power 1	−0.88	−0.70	146.35	140.50						
Power 2	−0.97	−1.00	143.92	137.89						
Power 3	−1.06	−1.23	143.42	137.18						
Power 4	−1.15	−1.41	144.07	137.61						
Co-kriging										
Stable	−0.41	−0.63	150.38	145.70	7.59	155.96	−0.053	−0.004	20.86	0.94
Spherical	−1.03	−0.60	151.24	145.62	173.90	165.31	−0.006	−0.004	0.87	0.88
Exponential	−1.18	−0.30	147.13	137.25	15.73	15.55	−0.078	−0.005	9.70	9.07
Gaussian	−0.41	−0.70	150.38	145.83	7.59	183.50	−0.053	−0.004	20.86	0.79
Ordinary kriging										
Stable	−0.59	−0.58	142.83	136.22	140.94	133.55	−0.003	−0.003	1.01	1.01
Spherical	−0.62	−0.58	143.37	136.87	141.04	133.41	−0.004	−0.003	1.01	1.02
Exponential	−0.60	−0.62	142.86	136.25	140.82	137.05	−0.003	−0.004	1.01	0.99
Gaussian	−0.63	−0.62	143.28	136.54	141.22	133.55	−0.004	−0.004	1.01	1.02

H high-temperature year, *L* low-temperature year

overestimation of the variance; if RMSS >1 or ASE < RMS, there is a tendency toward underestimation. The result interpolated by co-kriging with the spherical optimization model slightly overestimated the real NPP_{pot}. This has also been found in other studies. Li and Heap (2011) pointed out that kriging methods perform better than non-geostatistical methods, such as IDW, and co-kriging is better than ordinary kriging (Johnston et al. 2001; Li and Heap 2011; Scattolin et al. 2013). Above all, co-kriging is the best spatial interpolation method to predict the NPP_{pot}.

Comparing the NPP_{act} data

MODIS MOD17A3 NPP was used in this study as the actual NPP data. The MOD17A3 products derived from the moderate resolution imaging spectrometer (MODIS) and other sensors on the NASA Terra and Aqua platforms (Griffith et al. 2014) were used with the BIOME-BGC solar energy utilization model to build NPP prediction models to simulate the terrestrial ecosystem. These products are being used by scientists from a variety of disciplines, including oceanography, biology, and atmospheric science.

MODIS MOD17A3 NPP can retrieve the actual productivity (Conijn et al. 2013; Indiarto and Sulistyawati 2014) and has been widely used at the global and regional level (Zhao and Running 2010). Zhao et al. (2005) compared MODIS NPP with the ecosystem model-data intercomparison (EMDI) NPP data set and indicated that MOD17A3 is a more reliable product. MOD17A3 NPP data sets are now sufficiently mature to be used in a wide variety of applications, particularly where regularly, spatially referenced measures of vegetation activity are desired (Running et al. 2004). Zhao et al. (2005) found that the model used to calculate MOD17A3 is more reliable than other models, and the addition of annual GPP and meaningful annual QC make MOD17A3 more convenient for the community user. He also found that the global MODIS primary production data set is now ready to monitor ecological conditions, natural resources, and environmental changes. Consequently, this paper used MODIS NPP to calculate NPP_{act} of terrestrial ecosystem.

Further study

The proposed approach still needs improvement in the accuracy of identification and the extraction of natural vegetation in lower NPP areas. HI can be used in the areas that have high NPP with intense human activities, but it has a low accuracy in identifying and extracting natural vegetation in intense human activities with lower NPP. Further studies can focus on how to improve the accuracy of identification and extraction of natural vegetation in lower NPP areas.

The driving force of HI needs to be further studied. The change in HI is related to the land-use/land-cover change effects on ecosystems, such as forest converted to cultivated land or construction land. However, other factors also have a strong influence on NPP changes, e.g., climate change. Methods to remove the change in NPP that is due to climate change and find the driving force of the change in HI should be studied further.

Conclusions

Understanding and accurately assessing the risk human-induced land degradation poses to terrestrial ecosystem provides a scientific basis for promoting sustainable land use under the increasing pressure of population growth. There is a need for an indicator and corresponding method to quantify such hazardous impacts. This study proposed a hazardous impact indicator (HI) that can quantitatively express the negative effects of human-induced land degradation on terrestrial ecosystems. Hypotheses and procedures for quantifying HI were described in detail. The HI construction is completed in three steps: (1) extracting natural vegetation levels distributed in world- and national-level protected zones; (2) predicting potential productivity by using co-kriging based on the NPP of natural vegetation; and (3) calculating HI.

In the karst areas of south China, land with HI lower than 0.05 accounts for 43.47 %, meaning that more than half of this area is seriously affected by human-induced land degradation. Spatially, HI decreased from southwest to northeast. The highest HI areas were located in northwest Sichuan Province, southwest Yunnan Province, and the southern Guangxi Autonomous Region. A moderate HI area was located in southwest Guizhou Province. Low-HI areas were located in Hunan Province and Hubei Province. From 2000 to 2011, high-HI areas decreased yearly, and low-HI areas expanded, while high-HI areas increased after 2011. This is consistent with the period when the Grain-for-Green Project was in effect, indicating that land-use change due to human activity has a strong impact on KRD. To maintain a decreasing trend of HI, land-use policy will need to guide human activity.

In karst areas of south China, HI and rocky desertification are well matched in spatial distribution and intensity. The proposed HI approach proved to work well to assess hazardous impacts in regions where human activities play a leading role in land and ecological degradation, such as karst areas. However, many factors and human activities may cause NPP change. We therefore argue that NPP

reduction and HI do not follow a simple 1:1 relationship. Revisions may be needed when applying the proposed indicator and approach to other regions, and the approach still needs to improve its accuracy in identifying and extracting natural vegetation.

Acknowledgments Support from the National Key Research and Development Program (No. 2016YFA0602402), the National Basic Research Program of China: (Project Nos. 2012CB955403 and 2015CB954102), National Natural Science Foundation of China (Project No.: 41431177), Natural Science Research Program of Jiangsu(14KJA170001), PAPD, and National Key Technology Innovation Project for Water Pollution Control and Remediation (Project No.: 2013ZX07103006) and support from A-Xing Zhu through the Vilas Associate Award, the Hammel Faculty Fellow Award, the Manasse Chair Professorship from the University of Wisconsin-Madison, and the "One-Thousand Talents" Program of China are greatly appreciated.

References

Alves M, Carvalho L, Oliveira M (2013) Terrestrial Earth couple climate-carbon spatial variability and uncertainty. Glob Planet Change 111:9–30

Bai Z, Dent D, Olsson L et al (2008) Proxy global assessment of land degradation. Soil Use Manag 24:223–234

Bai Z, Conijn J, Bindraban P et al (2012) Global changes of remotely sensed greenness and simulated biomass production since 1981; towards mapping global soil degradation. ISRIC Report 2012/02. ISRIC, Wageningen

Bai X, Wang S, Xiong K (2013) Assessing spatial–temporal evolution processes of karst rocky desertification land: indications for restoration strategies. Land Degrad Dev 24:47–56

Blaikie P, Cannon T, Davis I et al (2014) At risk: natural hazards, people's vulnerability and disasters. Routledge, London

Boer M, Puigdefabregas J (2003) Predicting potential vegetation index values as a reference for the assessment and monitoring of dryland condition. Int J Remote Sens 24:1135–1141

Brandt J, Kuemmerle T, Li H et al (2012) Using Landsat imagery to map forest change in southwest China in response to the national logging ban and ecotourism development. Remote Sens Environ 121:358–369

Bridges E, Oldeman L (1999) Global assessment of human-induced soil degradation. Arid Soil Res Rehab 13:319–325. doi:10.1080/089030699263212

Burton I (1993) The environment as hazard. Guilford Press, New York

Cai Y (1996) Preliminary research on ecological reconstruction in karst mountain poverty areas of southwest. China Adv Earth Sci 11:602–606 **(in Chinese with English abstract)**

Cao S, Ma H, Yuan W et al (2014) Interaction of ecological and social factors affects vegetation recovery in China. Biol Conserv 180:270–277. doi:10.1016/j.biocon.2014.10.009

Conijn J, Bai Z, Bindraban P et al (2013) Global changes of net primary productivity, affected by climate and abrupt land use changes since 1981; towards mapping global soil degradation. ISRIC Report 2013/01, ISRIC-World Soil Information, Wageningen

Couckuyt I, Koziel S, Dhaene T (2013) Surrogate modeling of microwave structures using kriging, co-kriging, and space mapping. Int J Numer Model Electron Netw Dev Fields 26:64–73

Daily G (1995) Restoring value to the world's degraded lands. Science 269:350

de Jong R, de Bruin S, Schaepman M et al (2011) Quantitative mapping of global land degradation using earth observations. Int J Remote Sens 32:6823–6853

Diouf A, Lambin E (2001) Monitoring land-cover changes in semi-arid regions: remote sensing data and field observations in the Ferlo, Senegal. J Arid Environ 48:129–148

Du H, Peng W, Song T et al (2013) Plant community characteristics and its coupling relationships with soil in depressions between karst hills, North Guangxi, China. Chin J Plant Ecol 37:197–208 **(in Chinese with English abstract)**

Erb K, Haberl H, Jepsen M et al (2013) A conceptual framework for analysing and measuring land-use intensity. Curr Opin Environ Sustain 5:464–470. doi:10.1016/j.cosust.2013.07.010

Evans J, Geerken R (2004) Discrimination between climate and human-induced dryland degradation. J Arid Environ 57:535–554. doi:10.1016/S0140-1963(03)00121-6

Fasona M, Omojola A (2009) Land cover change and land degradation in parts of the southwest coast of Nigeria. Afr J Ecol 47:30–38

Fischer-Kowalski M, Haberl H (1998) Sustainable development: socio-economic metabolism and colonization of nature. Int Soc Sci J 50:573–587

Foley J, DeFries R, Asner G et al (2005) Global consequences of land use. Science 309:570–574

Ford DC, Williams PW (1989) Karst geomorphology and hydrology. Unwin Hyman, London

Friedl M, Sulla-Menashe D, Tan B et al (2010) MODIS Collection 5 global land cover: algorithm refinements and characterization of new datasets. Remote Sens Environ 114:168–182

Gong G, Mattevada S, O'Bryant S (2014) Comparison of the accuracy of kriging and IDW interpolations in estimating groundwater arsenic concentrations in Texas. Environ Res 130:59–69

Grau H, Aide T, Zimmerman J et al (2003) The ecological consequences of socioeconomic and land-use changes in postagriculture Puerto Rico. Bioscience 53:1159–1168

Griffith D, Ramkilowan A, Sprung D et al (2014) Exploration of satellite-derived data products for atmospheric turbulence studies. In: Comerón A, Kassianov E, Schäfer K et al (eds) Remote Sensing of Clouds and the Atmosphere XIX; and Optics in Atmospheric Propagation and Adaptive Systems XVII Society of Photo-Optical Instrumentation Engineers (SPIE) Conference Series, pp 1–14. doi:10.1117/12.2071893

Gutiérrez F, Parise M, De Waele J et al (2014) A review on natural and human-induced geohazards and impacts in karst. Earth Sci Rev 138:61–88

Haberl H, Erb K, Krausmann F et al (2001) Changes in ecosystem processes induced by land use: human appropriation of aboveground NPP and its influence on standing crop in Austria. Glob Biogeochem Cycles 15:929–942. doi:10.1029/2000gb001280

Haberl H, Fischer-Kowalski M, Krausmann F et al (2004a) Progress towards sustainability? What the conceptual framework of material and energy flow accounting (MEFA) can offer. Land Use Policy 21:199–213

Haberl H, Wackernagel M, Wrbka T (2004b) Land use and sustainability indicators. An introduction. Land Use Policy 21:193–198

Haberl H, Erb K, Krausmann F et al (2007) Quantifying and mapping the human appropriation of net primary production in earth's terrestrial ecosystems. Proc Natl Acad Sci USA 104:12942–12947. doi:10.1073/pnas.0704243104

Haberl H, Erb K, Krausmann F (2014) Human appropriation of net primary production: patterns, trends, and planetary boundaries. Annu Rev Environ Resour 39:363–391. doi:10.1146/annurev-environ-121912-094620

Haboudane D, Bonn F, Royer A et al (2002) Land degradation and erosion risk mapping by fusion of spectrally-based information and digital geomorphometric attributes. Int J Remote Sens 23:3795–3820

Hobbs R, Harris J (2001) Restoration ecology: repairing the earth's ecosystems in the new millennium. Restor Ecol 9:239–246

Huang Q, Cai Y, Xing X (2008) Rocky desertification, antidesertification, and sustainable development in the karst mountain region of Southwest China. AMBIO 37(5):390–392

Huang X, Lin D, Wang J (2013) Temporal and spatial NPP variation in the Karst region in south China under the background of climate change. Sci Silvae Sin 49:10–16 **(in Chinese with English abstract)**

Hutchinson G (1965) The niche: an abstractly inhabited hyper volume. In: Hutchinson G (ed) The ecological theater and the evolutionary play. Yale University Press, New Haven, pp 26–78

Indiarto D, Sulistyawati E (2014) Monitoring net primary productivity dynamics in Java island using MODIS satellite imagery. Asian J Geoinform 14:8–14

IUCN and UNEP-WCMC (2015) The world database on protected areas (WDPA) [on-line], [03/2015]. UNEP-WCMC, Cambridge. www.protectedplanet.net

Jiang B (2013) Head/tail breaks: a new classification scheme for data with a heavy-tailed distribution. Prof Geogr 65:482–494

Jiang Z, Lian Y, Qin X (2014) Rocky desertification in Southwest China: impacts, causes, and restoration. Earth Sci Rev 132:1–12

Johnston K, Ver Hoef JM, Krivoruchko K et al (2001) Using ArcGIS geostatistical analyst. ESRI, Redlands

Kennedy M, O'Hagan A (2000) Predicting the output from a complex computer code when fast approximations are available. Biometrika 87:1–13

Kiernan K (2010) Environmental degradation in karst areas of Cambodia: a legacy of war? Land Degrad Dev 21:503–519

Krausmann F, Haberl H, Schulz NB et al (2003) Land-use change and socio-economic metabolism in Austria—part I: driving forces of land-use change: 1950–1995. Land Use Policy 20:1–20

Krausmann F, Erb K, Gingrich S et al (2013) Global human appropriation of net primary production doubled in the 20th century. Proc Natl Acad Sci USA 110:10324–10329. doi:10.1073/pnas.1211349110

Kuemmerle T, Erb K, Meyfroidt P et al (2013) Challenges and opportunities in mapping land use intensity globally. Curr Opin Env Sustain 5:484–493. doi:10.1016/j.cosust.2013.06.002

Lei D, Shangguan Z, Rui L (2012) Effects of the grain-for-green program on soil erosion in China. Int J Sediment Res 27:120–127

Li W (2004) Degradation and restoration of forest ecosystems in China. For Ecol Manag 201:33–41

Li J, Heap A (2011) A review of comparative studies of spatial interpolation methods in environmental sciences: performance and impact factors. Ecol Inform 6:228–241

Li A, Wu J, Huang J (2012) Distinguishing between human-induced and climate-driven vegetation changes: a critical application of RESTREND in inner Mongolia. Landscape Ecol 27:969–982. doi:10.1007/s10980-012-9751-2

Lieth H (1975) Modeling the primary productivity of the world. In: Lieth H, Whittaker R (eds) Primary productivity of the biosphere. Springer, Berlin, pp 237–263

Liu T, Zhou G, Dan X (2009) Status quo, cause and prevention of karst stony desertification. Forestry Publishing House, Beijing **(in Chinese)**

Liu Y, Yu D, Su Y et al (2014) Quantifying the effect of trend, fluctuation, and extreme event of climate change on ecosystem productivity. Environ Monit Assess 186:8473–8486

Millennium Ecosystem Assessment (2005) Ecosystems and human well-being: synthesis. Island Press, Washington, DC

Monfreda C, Ramankutty N, Foley J (2008) Farming the planet: 2. Geographic distribution of crop areas, yields, physiological types, and net primary production in the year 2000. Global Boigeochem Cycles 22(GB1022):1–19. doi:10.1029/2007gb002947

Nel J, Le Maitre D, Nel D et al (2014) Natural hazards in a changing world: a case for ecosystem-based management. PLoS One 9:e95942. doi:10.1371/journal.pone.0095942

Nicholson S, Tucker C, Ba M (1998) Desertification, drought, and surface vegetation: an example from the West African Sahel. Bull Am Meteorol Soc 79:815–829. doi:10.1175/1520-0477(1998)079<0815:Ddasva>2.0.Co;2

Pan S, Tian H, Dangal S et al (2014) Complex spatiotemporal responses of global terrestrial primary production to climate change and increasing atmospheric CO_2 in the 21st century. PLoS One 9(11):e112810. doi:10.1371/journal.pone.0112810

Peng J, Wang Y, Wu J (2007) Human appropriation of net primary production: an approach for ecological assessment of regional sustainable development. J Nat Resour 22:153–158 **(in Chinese with English abstract)**

Plutzar C, Kroisleitner C, Haberl H et al (2016) Changes in the spatial patterns of human appropriation of net primary production (HANPP) in Europe 1990–2006. Reg Environ Change 16(5):1225–1238. doi:10.1007/s10113-015-0820-3

Prince S (2002) Spatial and temporal scales for detection of desertification. In: Reynolds JF, Stafford Smith D (eds) Global desertification: do humans cause deserts?. Dahlem University Press, Berlin, pp 23–40

Prince S, De Colstoun E, Kravitz L (1998) Evidence from rain-use efficiencies does not indicate extensive Sahelian desertification. Glob Change Biol 4:359–374. doi:10.1046/j.1365-2486.1998.00158.x

Prince S, Becker-Reshef I, Rishmawi K (2009) Detection and mapping of long-term land degradation using local net production scaling: application to Zimbabwe. Remote Sens Environ 113:1046–1057. doi:10.1016/j.rse.2009.01.016

Qi X, Wang K, Zhang C (2013) Effectiveness of ecological restoration projects in a karst region of southwest China assessed using vegetation succession mapping. Ecol Eng 54:245–253

Ramankutty N, Foley J (1999) Estimating historical changes in global land cover: croplands from 1700 to 1992. Glob Biogeochem Cycles 13:997–1027

Ray N, Adams J (2001) A GIS-based vegetation map of the world at the last glacial maximum (25,000–15,000 BP). Internet Archaeol 11(1):1–44. doi:10.11141/ia.11.2

Reynolds J, Stafford Smith D (2002) Global desertification: do humans cause deserts?. Dahlem University Press, Berlin

Reynolds J, Smith D, Lambin E et al (2007) Global desertification: building a science for dryland development. Science 316:847–851

Roberts D, Batista G, Pereira J et al (1999) Change identification using multitemporal spectral mixture analysis: applications in eastern Amazonia. In: Lunetta RS, Elvidge CD (eds) Remote sensing change detection: environmental monitoring methods and applications. Ann Arbor Press, Chelsea, pp 137–161

Running S, Nemani R, Heinsch F et al (2004) A continuous satellite-derived measure of global terrestrial primary production. Bioscience 54:547–560

Scattolin L, Bolzon P, Montecchio L (2008) A geostatistical model to describe root vitality and ectomycorrhization in Norway spruce. Plant Biosyst 142:391–400

Scattolin L, Alzetta C, Bolzon P et al (2013) Linden tree stress detection: chlorophyll–nitrogen contents and ectomycorrhizal community. Plant Biosyst 147:364–375

Shi P (2002) Theory on disaster science and disaster dynamics. J Nat Disasters 11(3):1–9 **(in Chinese with English abstract)**

Simard M, Pinto N, Fisher J et al (2011) Mapping forest canopy height globally with spaceborne lidar. J Geophys Res: Biogeosciences 116(G04021):1–12

Sorrensen C (2009) Potential hazards of land policy: conservation, rural development and fire use in the Brazilian Amazon. Land Use Policy 26:782–791

State Forestry Administration of China (2012) Chinese Rocky Desertification Bulletin. http://www.forestry.gov.cn/uploadfile/zsxh/2012-6/file/2012-6-18-8add268dbe3c4180b10408ead795d23c.pdf. Accessed 23 July 2016

State Forestry Administration of China (2013) National Forest Park Directory. http://www.forestry.gov.cn/portal/slgy/s/2452/content-684348.html. Accessed 31 December 2015

Sweeting M (2012) Karst in China: its geomorphology and environment. Springer, Berlin

Tian Y, Haibara K, Toda H et al (2008) Microbial biomass and activity along a natural pH gradient in forest soils in a karst region of the upper Yangtze River, China. J For Res Jpn 13:205–214. doi:10.1007/s10310-008-0073-9

Tilman D, Cassman K, Matson P et al (2002) Agricultural sustainability and intensive production practices. Nature 418:671–677

Tobler W (1970) A computer movie simulating urban growth in the Detroit region. J Econ Geogr 234–240

Uchida E, Xu J, Rozelle S (2005) Grain for green: cost-effectiveness and sustainability of China's conservation set-aside program. Land Econ 81:247–264

UNCCD (1993) Agenda 21: earth summit—the United Nations programme of action. United Nations, New York

UNCCD (1994) United Nations Convention to Combat Drought and Desertification in Countries Experiencing Serious Droughts and/or Desertification, Particularly in Africa. http://www.unccd.int/Lists/SiteDocumentLibrary/Publications/UNCCD_Convention_ENG.pdf. Accessed 30 Mar 2016

Vitousek P, Mooney H, Lubchenco J et al (1997) Human domination of earth's ecosystems. Science 277:494–499. doi:10.1126/science.277.5325.494

Wang S, Liu Q, Zhang D (2004) Karst rocky desertification in southwestern China: geomorphology, landuse, impact and rehabilitation. Land Degrad Dev 15:115–121

Wang G, Innes J, Lei J et al (2007) China's forestry reforms. Science 318:1556–1557

Wang K, Zhang C, Li W (2013) Predictive mapping of soil total nitrogen at a regional scale: a comparison between geographically weighted regression and cokriging. Appl Geogr 42:73–85

Wessels K, Prince S, Frost P et al (2004) Assessing the effects of human-induced land degradation in the former homelands of northern South Africa with a 1 km AVHRR NDVI time-series. Remote Sens Environ 91:47–67. doi:10.1016/j.rse.2004.02.005

Wessels K, Prince S, Malherbe J et al (2007) Can human-induced land degradation be distinguished from the effects of rainfall variability? A case study in South Africa. J Arid Environ 68:271–297. doi:10.1016/j.jaridenv.2006.05.015

Wessels K, Prince S, Reshef I (2008) Mapping land degradation by comparison of vegetation production to spatially derived estimates of potential production. J Arid Environ 72:1940–1949

Wessels K, Van Den Bergh F, Scholes R (2012) Limits to detectability of land degradation by trend analysis of vegetation index data. Remote Sens Environ 125:10–22

Williams P (1993) Environmental change and human impact on karst terrains: an introduction. Catena 25:1–19

Williams P (2008) World heritage caves and karst. IUCN, Gland, p 57

Xiao H, Weng Q (2007) The impact of land use and land cover changes on land surface temperature in a karst area of China. J Environ Manage 85:245–257. doi:10.1016/j.jenvman.2006.07.016

Xiong Y, Qiu G, Mo D et al (2009) Rocky desertification and its causes in karst areas: a case study in Yongshun County, Hunan Province, China. Environ Geol 57:1481–1488. doi:10.1007/s00254-008-1425-7

Xu D, Kang X, Zhuang D et al (2010) Multi-scale quantitative assessment of the relative roles of climate change and human activities in desertification—a case study of the Ordos Plateau, China. J Arid Environ 74:498–507

Yue Y, Wang K, Liu B et al (2013) Development of new remote sensing methods for mapping green vegetation and exposed bedrock fractions within heterogeneous landscapes. Int J Remote Sens 34:5136–5153

Zeng F, Peng W, Song T et al (2007) Changes in vegetation after 22 years' natural restoration in the Karst disturbed area in northwestern Guangxi, China. Acta Ecol Sin 27:5110–5119

Zhang J, Kalacska M, Turner S (2014) Using landsat thematic mapper records to map land cover change and the impacts of reforestation programmes in the borderlands of southeast Yunnan, China: 1990–2010. Int J Appl Earth Obs Geoinf 31:25–36

Zhao M, Running S (2010) Drought-induced reduction in global terrestrial net primary production from 2000 through 2009. Science 329:940–943

Zhao M, Heinsch F, Nemani R et al (2005) Improvements of the MODIS terrestrial gross and net primary production global data set. Remote Sens Environ 95:164–176. doi:10.1016/j.rse.2004.12.011

Zhou W, Gang C, Zhou F et al (2015) Quantitative assessment of the individual contribution of climate and human factors to desertification in northwest China using net primary productivity as an indicator. Ecol Indic 48:560–569. doi:10.1016/j.ecolind.2014.08.043

Zika M, Erb K (2009) The global loss of net primary production resulting from human-induced soil degradation in drylands. Ecol Econ 69:310–318